Biosensors and Bioelectronics 25 (2010) 2343–2350

Contents lists available at ScienceDirect

Biosensors and Bioelectronics

journal homepage: www.elsevier.com/locate/bios

# A single carbon fiber microelectrode with branching carbon nanotubes for bioelectrochemical processes

Xueyan Zhao[a,b], Xin Lu[a,b], William T.Y. Tze[a,**], Ping Wang[a,b,*]

[a] Department of Bioproducts and Biosystems Engineering, Biotechnology Institute, University of Minnesota, St. Paul, MN 55108, USA
[b] Biotechnology Institute, University of Minnesota, Saint Paul, MN 55108, USA

ARTICLE INFO

*Article history:*
Received 13 January 2010
Received in revised form 19 March 2010
Accepted 24 March 2010
Available online 1 April 2010

*Keywords:*
Carbon fiber microelectrode
NADH oxidation
Glycerol oxidation
Glycerol dehydrogenase detection
Carbon nanotubes modified electrode

ABSTRACT

Carbon fiber electrodes are greatly promising for microelectronic applications including high performance biosensors, miniaturized transmitters, and energy storage and generation devices. For biosensor applications, one drawback of using carbon fiber microelectrodes, especially single fiber electrodes, is the weak electronic signals, a consequence of low surface area of fibers, which ultimately limit the sensitivity of the sensors. In this paper, we report a novel single fiber microelectrode with branched carbon nanotubes for enhanced sensing performance. The fiber microelectrode was prepared from carbonization of cellulose fibers. Upon introduction of carbon nanotubes, the carbon fibers exhibited a significant increase in the specific surface area from <10 to 36.4 $m^2/g$ (determined by the BET method). A single fiber electrode with such a hierarchical structure was examined for redox reactions of coenzyme NAD(H) which is useful to mediate the assays and transformations of a broad range of biochemicals. Experimental results showed that carbon nanotubes enhanced the redox reactions on surfaces of the electrode by reducing the oxidation potential of NAD(H) from 0.8 to 0.55 V. The single carbon fiber with branched nanotubes was also examined for the detection of glycerol, and the results showed linear responding signals in a concentration range of 40–250 μM. These results are comparable to the properties of fossil-based carbon materials, and thus our cellulose-based carbon electrodes provide a potentially sustainable alternative in bioelectrochemical applications.



## 1. Introduction

Single carbon fiber electrodes are greatly promising for microelectronic applications including high performance biosensor (Štulík et al., 2000) and miniaturized energy devices such as fuel cells (Mano et al., 2003). For sensor applications, single carbon fiber electrodes are especially appealing in that they require only a small amount of samples, but provide high signal/noise ratios and render short responding times (Amatore and Maisonhaute, 2005; Baltes et al., 2004; Wightman, 1988). Such sensors have found a variety of applications. For example, single carbon fiber electrodes have been applied for measurements of real time chemical release from single cells (Amatore et al., 2008; Du et al., 2008) and as neurotransmitters for *in vivo* monitoring of signal generation in brain cells (Bruns, 2004; Robinson et al., 2008).

One drawback in using carbon fiber microelectrodes is that they provide only a limited surface area and thus very weak electronic signals which require very sensitive instrumental detection. This setback is a result of the small diameter of carbon fibers that ranges from several micrometers to tens of micrometers. One way to overcome this drawback is to deposit carbon nanotubes (CNTs) on the fiber surface to improve the overall surface area without substantially changing the size of the electrode. CNT deposition had been attempted on single carbon fiber microelectrode (Wang et al., 2005) and nanoelectrode (Chen et al., 2003) by dipping carbon fiber electrodes into CNT suspension with the aid of dispersing agents, such as surfactant (sodium dodecyl sulfate). Suspensions of CNTs in Nafion® solution were also used for CNT deposition on electrode by dip-coating (Swamy and Venton, 2007) and by electrochemical deposition (Du et al., 2008). In addition to improving specific surface areas, CNTs also impart many favorable electronic properties desired for high performance biosensing and nano-electronic fabrication (Sgobba and Guldi, 2009). CNTs have also been found capable of promoting electron-transfer reactions, minimizing fouling of electrode surfaces (Nowall and Kuhr, 1995), enhancing electrocatalytic activity, and facilitating the immobilization of enzymes and antibodies on the surface of electrodes (Valcarcel et al., 2007; Wang et al., 2007).

* Corresponding author at: Department of Bioproducts and Biosystems Engineering, University of Minnesota, 2008 Folwell Ave., Saint Paul, MN 55108, USA. Tel.: +1 612 624 4792; fax: +1 612 625 6286.
** Corresponding author. Tel.: +1 612 624 2383; fax: +1 612 625 6286.
*E-mail addresses:* wtze@umn.edu (W.T.Y. Tze), ping@umn.edu (P. Wang).

0956-5663/$ – see front matter © 2010 Elsevier B.V. All rights reserved.
doi:10.1016/j.bios.2010.03.030

As such, CNT-fabricated carbon fiber microelectrodes have been examined for biosensors (Huffman and Venton, 2009; Zayats et al., 2008), micro-column separation (Aguei et al., 2008), and biofuel cells (Kim et al., 2008).

Advances were made on preparing and using CNT-containing electrodes for oxidation of NADH but the advantages of CNTs have yet to be more fully tapped. Viry et al. (2007) reported a method for producing CNT fibers by co-electrospinning CNT with poly (vinyl alcohol) polymer, followed by a heat-treatment procedure to remove the polymer, producing fibers in the form of CNT bundles. Such CNT fibers were used as micro disk electrodes and examined for glucose assay, and were found able to offer improved activities for the oxidation of NADH as compared to single carbon fiber electrodes. In another effort, similar CNT fibers were prepared by a simple particle-coagulation spinning process, involving the injection of a homogeneous CNT dispersion in a polymer solution, and the produced fibers have an interconnected CNT/polymer-chain network (Vigolo et al., 2000). Such CNT-containing fiber microelectrodes exhibited good electrocatalytic activities and effectively reduced the NADH oxidation potential by ~0.2 V (Wang et al., 2003). To our opinion, the above-mentioned preparation of CNT-containing electrodes does not promise to fully capitalize the potentials of CNTs, as the fabrications generally led to CNTs that are bundled together or embedded inside other supports such as polymers, exposing only a portion of CNTs for reactions.

In the current work we explore the use of carbon fiber and CNT hierarchical electrodes with the nanotubes branched out from the surface of the fibers, to generate CNT structures with surfaces fully exposed for interactions with surrounding solutions. Previous studies of carbon fiber electrode fabrication based on fossil-based polymers lack the potential of sustainability. A feasible approach could be carbonization of renewable materials from biomass. Cellulose, the most abundant polymeric constituent in biomass, is composed of β-D glucopyranose units which are linked together in linear chains by 1–4 glycosidic bonds. The pyranose units, upon pyrolysis, are dehydrated to a carbonaceous polymer intermediates which can be transformed into a polyaromatic structure (Plaisantin et al., 2001), constituents characteristic of carbon materials. Indeed, many published studies have reported the production of carbon fibers from cellulose fibers in the form of native cellulose (e.g. Kim et al., 2001) and extruded regenerated cellulose fibers (e.g. Peng et al., 2003). Hierarchical porous carbon structures have also been transformed through pyrolysis of cellulose acetate filters used in cigarettes (Polarz et al., 2002). These cellulose carbonization processes, however, were not aimed at electrochemical applications.

There have been so far no reported attempts in growing CNTs on surfaces of cellulose-derived carbon fibers to produce nanostructure materials. Metal-catalyzed growth of nanotubes has been applied widely in recent years for preparing a variety of nanostructured materials, such as the fiber–tube and fiber–fiber (Li et al., 2009) hybrid carbon materials, for the purposes of increasing surface area, providing higher sensitivities and ease of preparation for many applications including field effect transistors (Qu et al., 2008). The introduction of CNTs in this kind of nanostructured materials for electrochemical applications has resulted in a great improvement in electrochemical properties. All of these reported CNT growth are on fossil-based materials, and it is therefore necessary to investigate the use of renewable materials for sustainable production of CNT-based electrodes.

This work explored the use of cellulose materials for preparation of hierarchical carbon materials. A new and facile fabrication production method of CNT-carbon fibers was developed through carbonization of cellulose fibers and growth of CNT in the presence of Fe. A single CNT-modified carbon fiber was then used as a microelectrode, and tested for the efficiency of oxidation reaction of NADH generated from the glycerol oxidation reaction to explore its potential in large-scale electrochemical applications involving NADH reuse and regeneration. It is expected that the single CNT-modified carbon fiber from cellulose will provide sensitive detection corresponding to the concentration changes of NADH in glycerol oxidation reaction, lower the potential of NADH oxidation on carbon electrode and reduce the electrode fouling.

## 2. Chemicals and methods

### 2.1. Production of CNT-modified carbon microfiber

Cellulose fibers, acquired as medical grade cotton wool (Weng Thye Heng SDN BHD, Penang, Malaysia), were pre-treated before modifying with CNTs. The pre-treatment was performed by dipping the cellulose wool pad ($2 \times 2''$) into 50 ml of well suspended dimethylformamide solution containing 3.3 wt% of Fe (III) acetylacetonate ($Fe(C_5H_7O_2)_3$ (>99.9%, Aldrich, St. Louis, MO, USA) for 2 h at room temperature. The pre-treated sample was dried at room temperature in a convection-flow fume hood for overnight before carbonization. Carbonization and CNT modification were performed in a high temperature tubular furnace (Sentro Tech., Model STT-1200-3.5-12, Cleveland, OH, USA) with a procedure adopted from reference Hou and Reneker (2004) with modification. In a typical preparation, the furnace chamber was first purged with argon at a flow rate of 450 ml/min for 30 min. After loading the pre-treated cellulose wool pad, the sample was annealed at 250 °C for 3 h. The $Fe^{3+}$ ions loaded on the cellulose fibers were reduced to Fe by introducing hydrogen into the furnace chamber at a flow rate of 150 ml/min for 4 h at 500 °C in the argon atmosphere. The cellulose fibers were then carbonized at 850 °C for 30 min. For carbonization of cellulose fibers without CNT growing, the above-mentioned steps were repeated except for the pre-treatment step. For growing CNTs on carbon fibers, the furnace temperature were cooled down from 850 to 700 °C, and hexane vapor was subsequently added at a flow rate of 600 ml/min with argon as the carrier gas. The hexane served as a carbon source for CNTs, whose desired length was controlled by the hexane feeding time, which is in the range of 3–20 min.

The morphology of carbonized samples was studied by using scanning electron microscopy (Hitachi S3500N Variable Pressure SEM) and transmission electron microscopy (Philips CM12 Transmission Electron Microscope). The surface areas of samples were determined by using gas sorptometer (ASAP, 2000, Micromeritics, Norcross, GA, USA) based on physical adsorption of nitrogen gas molecules. The adsorption isotherm was analyzed using the BET method (Brunauer et al., 1938) to calculate for the quantity of gas involved in the monolayer coverage of material surfaces, thereby allowing estimation of specific surface area. All measurements above were preformed in accordance with standard sample preparation protocols.

### 2.2. Fabrication of carbon fiber microelectrode

One single carbon fiber (modified with or without CNTs) was pulled out from the carbonized sample pad, and glued with a conductive carbon paint (SPI supplies, West Chester, PA, USA) onto a copper wire ($L = 85$ mm) inserted through a capillary (Drummond Scientific Company, Broomall, PA, USA). Both ends of the capillary tube were sealed with epoxy glue (Armstrong Products Company, Easton, MA, USA). The exposed fiber length was measured under an optical microscope, and controlled by trimming to 3 mm. The resulting microelectrodes are named carbon fiber microelectrode (CFME) and CNT-carbon fiber microelectrode (CNT-CFME). After drying at room temperature for overnight, the fabricated carbon fiber microelectrode was used in the following electrocatalytic measurements.

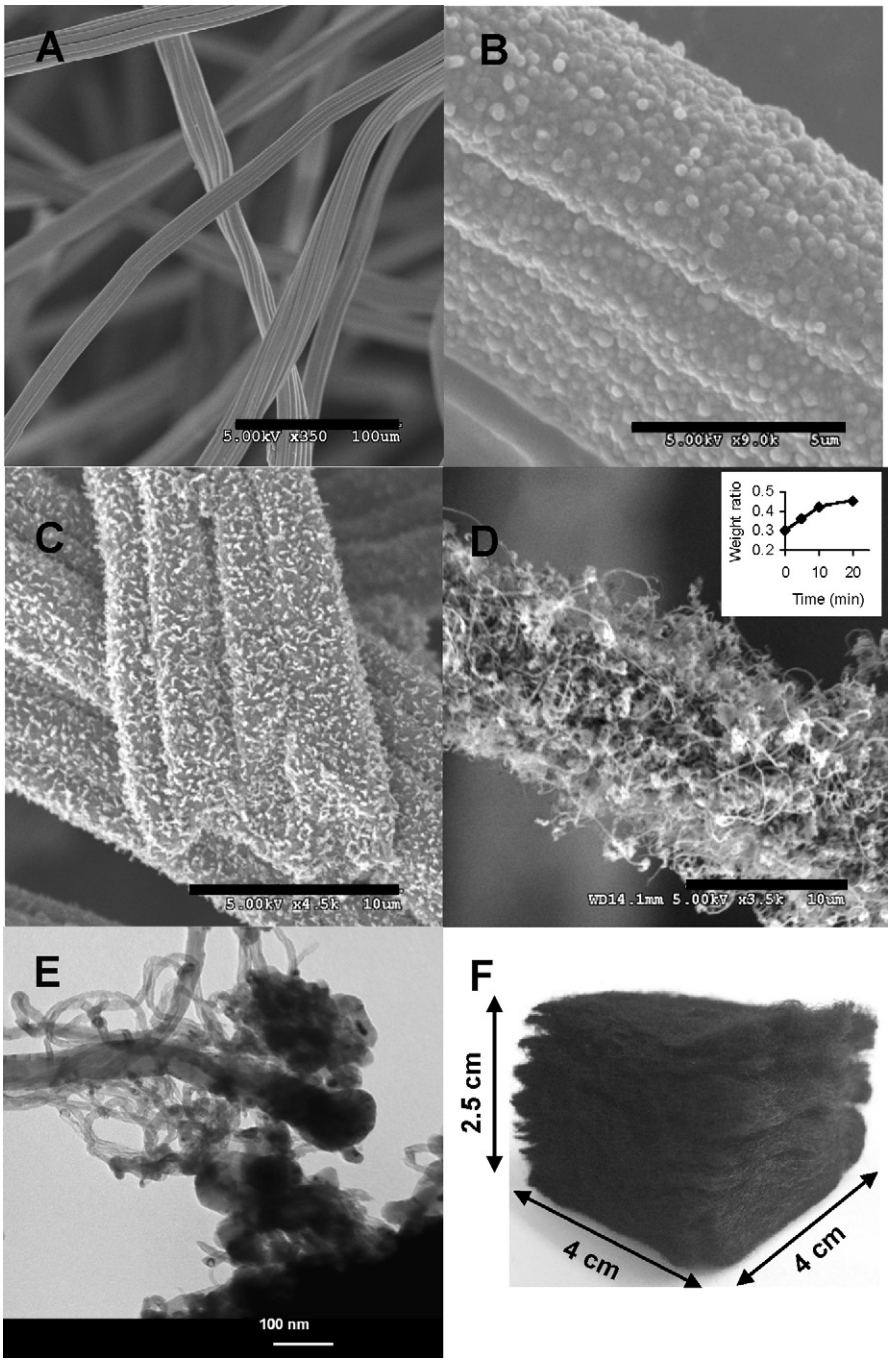


**Fig. 1.** Images of carbonized fiber and CNT coated carbon fiber. (A) SEM of cellulose fibers, scale bar: 100 μm; (B) SEM of reduced Fe particles on the surface of a cellulose fiber, scale bar: 5 μm; (C) SEM of CNT-enabled carbonized fibers with 5 min of hexane feed, scale bar: 10 μm; (D) SEM of a CNT-enabled carbonized fiber with 20 min of hexane feed, scale bar: 10 μm; inset: weight percentage based on original sample weight *vs*. carbonization time; (E) TEM of a suspension of CNT in ethanol/$H_2O$ mixture showing two different sizes of CNT diameter (~100 nm and ~10 nm), scale bar: 100 nm; (F) photo of a 3-D structured carbonized fiber material.

### *2.3. Electrocatalytic studies of carbon fiber microelectrodes*

The electrochemical properties of microelectrodes were tested by using the CHI 760C electrochemical workstation (CH Instruments, Inc., Austin, TX, USA) with a three-electrode system. The CFME or CNT-CFME sample was used as the working electrode. The Ag/AgCl electrode and Pt wire electrode were used as the reference and counter electrodes, respectively. The effective electrocatalytic surface area of each microelectrode was measured by using cyclic voltammetry at different scan rates (0.01–0.3 V/s) with $K_3Fe(CN)_6$ as electrolyte in 0.1 M KCl. The oxidation of NADH on CFME and CNT-CFME was investigated by cyclic voltammetry of 0.5 mM NADH (Sigma, St. Louis, MO, USA) in 0.05 M $NH_4Cl$–$NH_4OH$ buffer (pH 9.0). When CFME or CNT-CFME was applied in the regeneration of NAD in the oxidation reaction of glycerol, 4 ml of a total reaction system containing 25 mM of glycerol (Sigma, St. Louis, MO, USA), 0.24 U/ml of glycerol dehydrogenase (Sigma, St. Louis, MO, USA), and various concentrations of NAD ranging from 0 to 2 mM were used.

## 3. Results and discussions

This work examined the growth of CNTs on the surface of carbonized cellulose fibers. The cellulose fiber is shown in Fig. 1A.

Controlled growth of carbon nanotubes on fiber surfaces was realized via deposition of metal particles without addition of dispersing aids. When the cellulose fibers were deposited with $Fe^{3+}$ salt (pretreatment) followed by carbonization at 850 °C for 30 min and reduction by introducing $H_2$ gas into the furnace chamber, the Fe salts were reduced to Fe particles. The carbonized fibers prior to CNT growth maintained 30.3% of the original weight, and the reduced Fe particles on the carbonized fiber surface are shown in Fig. 1B. On the other hand, the carbonized fibers without loading of Fe salt weighed 26.5% of the original weight after undergoing the same procedure of carbonization, thus the deposited metal particle amounted to 3.8% of the cellulose weight.

The growth and morphology of CNT-carbon fibers are evidenced from the SEM images. After cellulose fibers were loaded with the Fe precursor, a continuous thin film was uniformly coated onto the whole surface (data not shown). During the reduction of $Fe^{3+}$ to Fe with $H_2$, different sizes of iron particles were formed on the surface of carbonized fiber surface (Fig. 1B). Since the surface of cellulose fiber is not as smooth as shown in Fig. 1A, the Fe particles were not uniformly formed. Individual cellulose fibers have an average diameter of ~20 μm (Fig. 1A), which was reduced to ~15 μm after carbonization, suggesting a loss of material as reported in another study on cellulose carbonization (Kim et al., 2001). Upon CNT growth, however, the diameter of individual fibers was reduced to a range of 10–15 μm. This diameter decrease could be attributed to the prolonged heat exposure during the CNT growing stage, causing a diameter shrinkage that prevailed over the diameter gain from the grown (protruded) CNTs. The hexane supply time influenced the length of CNTs grown on the carbonized fiber surfaces. A longer hexane exposure time resulted in longer CNTs (Fig. 1C and D).

The CNT-grown carbon fibers exhibited a weight gain that corresponds to the increased CNT length. The weight of (CNT-enabled) carbon fibers, as a percentage of the starting cellulose fibers, increased linearly (from 30.3% to 42.2%) at the first 10 min of hexane exposure. The weight gain slowed down after 10 min, with a weight ratio of 45.4% at 20 min. This observation could be attributed to the limited space adjacent to the fiber surface for CNTs at high growth density.

The CNT-carbon fibers prepared was further investigated under TEM. Samples of these fibers were first suspended in an ethanol/$H_2O$ mixture and sonicated for 2 min. Under TEM, coiled and branched CNTs were observed on the surface of carbon fibers, with the iron particle core on the tips of CNTs (Fig. 1E), verifying that CNT growth were enabled at the catalysts locations. This observation is in agreement with previously reported CNT growth on synthetic electrospun polyacrylonitrile (PAN) fibers (Hou and Reneker, 2004) in which CNTs were grown at the location where catalysts exist. Branched CNTs grown on the surface of a carbon fiber were shown in Fig. 1E. Two different diameters of CNT were found (~100 nm and ~10 nm), and the thinner CNTs were not observable from SEM images. These TEM results also indicated that the Fe precursor formed different sizes of particles during reduction, but only the large Fe particles could be observed under SEM. The TEM images also revealed that thinner CNTs (~10 nm) are hollow and branched, while thicker (~100 nm) CNTs are on the surface of carbon fiber. A similar anchorage of carbon nanofibers on structured carbon microfibers was also reported (Li et al., 2009). However, this previous study reported growth of nanofibers on the surface of carbon microfibers, while our present study clearly demonstrates the growth of carbon nanotubes.

In a bigger dimensional scale, the CNT-modified carbon fibers produced in this study are a 3-D structured material (Fig. 1F). Our success in producing such materials from renewable fibers strongly contrasts other research with CNT growth, which was conducted on fossil-based fibers (Hou and Reneker, 2004). In addition to the size shown in Fig. 1F, different geometries of materials can also be produced with the same protocol.

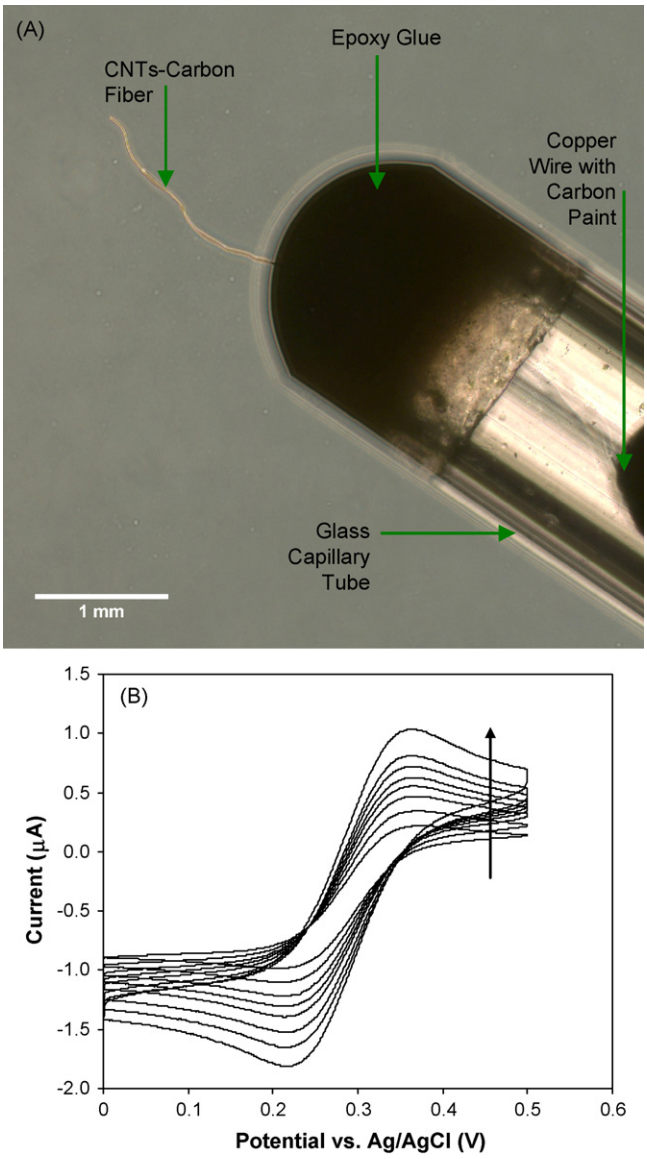


**Fig. 2.** Image and cyclic voltammograms of a fabricated CNT-CFME electrode. (A) Microscopic image of CNT-CFME electrode; (B) cyclic voltammograms of the CNT-Carbon Fiber Microelectrode (CNT-CFME) in 0.1 M KCl solution containing 4 mM $K_3Fe(CN)_6$, at different scan rates (0.01, 0.025, 0.05, 0.075, 0.1, 0.15, 0.2 and 0.3 V/s). Arrow in the figure indicates increasing scan rates.

To investigate surface areas of the carbonized samples, two samples were selected (carbonized fibers and CNT-carbon fibers) for the BET measurement. The BET surface area of blank carbon fibers was below the measurement limit (10 $m^2/g$). The BET result for CNT-carbon fiber was $36.4 \pm 0.2$ $m^2/g$, thus showing a dramatic increase in the surface area with the growth of CNTs on carbonized fibers. This surface area is comparable to the reported data (23 $m^2/g$) for CNT grown on carbon felt (Li et al., 2009) for 1–9 h.

In addition to BET surface area of bulk samples, the effective surface area of single fibers available for electrochemical reaction was measured by using cyclic voltammetry. Samples (Fig. 2A) of the carbon fiber microelectrode (CFME) and CNT-carbon fiber microelectrode (CNT-CFME) were tested at different scan rates in 4 mM of $K_3Fe(CN)_6$ in 0.1 M of KCl solution. Results are shown in Fig. 2B. The effective surface area of CFME and CNT-CFME were calculated

based on the Randles Sevich equation (Brett and Brett, 1993):

$$I_p = 2.69 \times 10^5 n^{3/2} A C D^{1/2} \nu^{1/2}, \quad (1)$$

where $n$ is the electron numbers transferred, in this case $n = 1$ for $K_3Fe(CN)_6$; $A$ is the electrode surface area; $C$ is the concentration of $K_3Fe(CN)_6$; $D$ is the diffusion coefficient of $K_3Fe(CN)_6$, which is $7.62 \times 10^{-6}$ cm$^2$/s in 0.1 M KCl solution (Walters et al., 1984); $\nu$ is the scan rate in cyclic voltammetry.

Values of the effective surface area of single CFME and CNT-CFME calculated the Randles Sevich equation were, respectively, $2.0 \times 10^{-4}$ and $2.6 \times 10^{-4}$ cm$^2$/mm. The fiber surface area/volume could be estimated from the length (1 mm) of the exposed fiber and the fiber diameter (11.2 μm for CFME, and 14.4 μm for CNT-CFME) determined from SEM. Results showed that the surface area of CFME and CNT-CFME were $1.2 \times 10^5$ and $2.7 \times 10^5$ m$^2$/m$^3$, respectively, suggesting an over two-fold increase in the effective electrode surface area. Such an increase is less compared to the BET measurement which revealed more than three-fold enhancement in specific surface area. The disparity can be explained by the difference in diffusion patterns between the $K_3Fe(CN)_6$ used in cyclic voltammetric measurements and the nitrogen gas used in BET adsorption measurements. Since smaller molecules such as nitrogen can diffuse into smaller pores, more surface area is detected in BET measurements. Indeed, the BET measurement gave an average pore size of 9.67 nm in the presence of thinner CNTs, and this pore size is large enough for the diffusion of small molecules.

Since carbonized fibers in this study will be used in electrochemical applications, electrical conductivity is a very important factor to study. Conductivity results of the carbonized fiber and CNT-enabled carbonized fiber were, respectively, calculated to be $3030 \pm 550$ S/m and $4592 \pm 828$ S/m by measuring the current passing through a single fiber when a known voltage was applied. The electrical conductivity of polyacrylonitrile (PAN) based electrospun fiber and the CNT-PAN nanofiber were reported, respectively, to be 480 S/m (Wang et al., 2002) and 1315 S/m (Hou and Reneker, 2004). The conductivity of our carbonized fiber is over six-folds higher than that of the electrospun PAN fiber, indicating that carbonized cellulose fibers have the potential to be widely used in electrocatalytic area. When branched CNTs were grown on the surface of the carbonized cellulose fiber, the conductivity increased another 1.5 times.

CFME and CNT-CFME electrodes were used as working electrodes in a three-electrode electrochemical setup for detecting the oxidation of NADH. NADH is the reduced form of nicotinamide adenine dinucleotide (NAD), an important electroactive biomolecule. The NAD/NADH is shared by over 400 dehydrogenase enzymes as cofactor (Nowall and Kuhr, 1995). In bioelectrochemical applications, the recycling of NADH to NAD is important for the purpose of sustainability. The direct oxidation of NADH to NAD was hardly realized on traditional electrodes, such as gold, platinum, and glassy carbon electrode, due to the high overpotential (>1.0 V) caused by sluggish charge transfer kinetics (Jaegfeldt, 1980; Moiroux and Elving, 1978) and electrode fouling by the adsorption of NADH and the produced NAD (Hayes and Kuhr, 1999). CNT-based electrodes illustrated the possibility of reducing the oxidation potential of NADH, and the catalytic ability on the oxidation of NADH was reported to improve for electrodes modified with CNTs (Kumar and Chen, 2008).

In the present work the different oxidation properties of NADH on CFME and CNT-CFME were first investigated by cyclic voltammetry in the presence/absence of 0.5 mM NADH in 0.05 M $NH_4Cl$–$NH_4OH$ buffer (pH 9.0). As shown in Fig. 3, both electrodes showed catalytic ability for the oxidation of NADH without the presence of any mediators. However, the oxidation current of NADH started to increase after the potential reached 0.45 V on CFME, while the increase in current started right after the potential reached

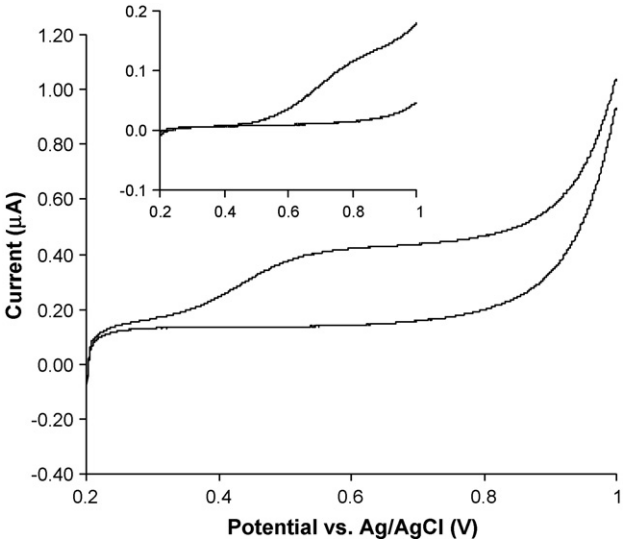


**Fig. 3.** Oxidation curves of cyclic voltammograms on the CNT-Carbon Fiber Microelectrode (CNT-CFME) and Carbon Fiber Microelectrode (CFME, inset) in 0.5 mM NADH solution (pH 9.0) contained in 50 mM $NH_4Cl$–$NH_4OH$ buffer (pH 9.0); scan rate 100 mV/s.

0.2 V on CNT-CFME. The result for CNT-CFME is comparable to the previously published oxidation potential (+0.4 V) of heat treated multi-walled carbon nanotubes fiber microelectrode (Wang et al., 2003). The higher surface area and the presence of CNTs served to facilitate the oxidation of NADH on carbon fiber electrode and to lower the overpotential. When the potential of both electrodes was at 0.6 V, the oxidation current of NADH on CNT-CFME was 0.28 μA, which is over 10 times higher than that on CFME. From the cyclic voltammograms, we also observed that the current became stabilized at the potential range of 0.55–0.78 V, thus allowing us to conclude that within this potential range, the oxidation rate of NADH on the surface of CNT-CFME was in equilibrium with the diffusion rate of NADH to the electrode surface.

The oxidation of NADH on CNT-CFME was investigated by examining currents generated in cyclic voltammetry and amperometry, respectively. As shown in Fig. 4A the oxidation currents of NADH in both measurements were closely agreeable, and the linear range for NADH detection is up to 2.5 mM. The detection limit of CNT-CFME electrode was 0.008 mM for NADH, which is slightly lower than the 0.01 mM reported in the literature on a polymer-modified carbon fiber electrode (Ju and Leech, 1997). A typical current response to changes of NADH concentrations is shown in Fig. 4B. From the amperometry experiment, the current response time was ~14 s, i.e. it took about 14 s for the current to reach 95% of the stable reading.

The highly sensitive and efficient redox reaction of NADH could be applied to many bioassays that involve the activity of NADH. We explored in this work the reaction of glycerol oxidation catalyzed by glycerol dehydrogenase. The glycerol oxidation reaction was carried out in a 4-ml three-electrode electrochemical cell, with the CNT-CFME electrode as the working electrode, and Ag/AgCl and Pt wire electrodes as the reference and counter electrodes, respectively. The reaction was conducted at initial concentrations of 50 mM of glycerol, 2 mM of NAD, and 26.7 U/ml of glycerol dehydrogenase. The time course of NADH concentrations (Fig. 5A) in the reaction system was recorded from the increasing peak current at 0.55 V in cyclic voltammograms in a non-stirring system. The potential was selected to be 0.55 V based on the high oxidation current of NADH in the range of 0.55–0.78 V as observed from cyclic voltammogram. Fig. 5A shows that the current increased linearly with time for the first 10 min, thus exhibiting the concentration of product–time relationship at the initial reaction of

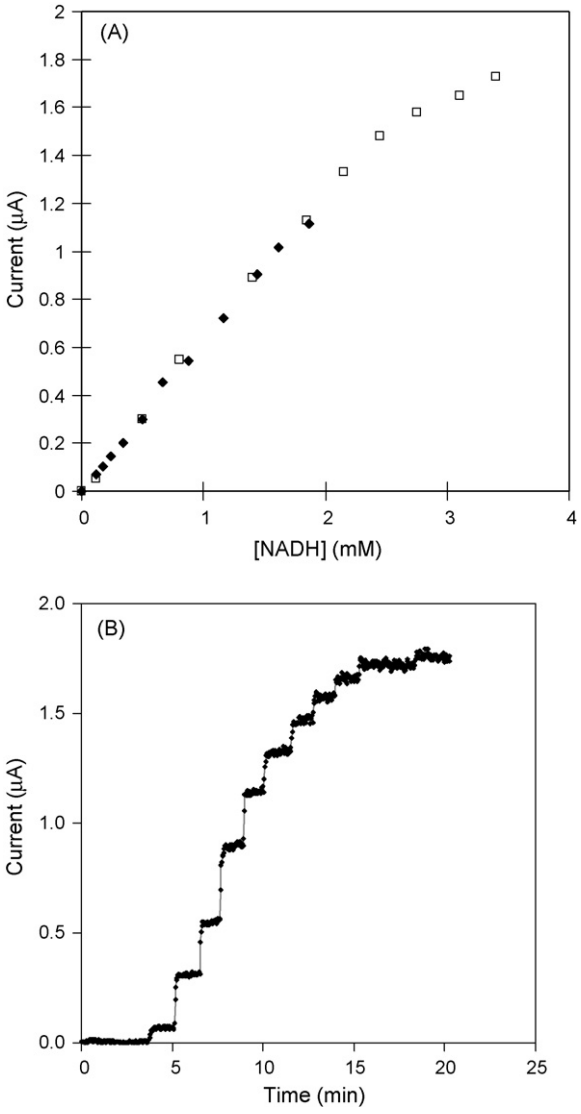


**Fig. 4.** Current responses in detecting NADH. (A) Current of NADH oxidation to the change of NADH concentration on cyclic voltammogram (CV) and amperometry. Filled diamond (♦): current reading from CV; Open square (□): current reading from I-t; (B) Typical current response to NADH concentration in amperometry without stirring. Aliquot of NADH solution was injected to the electrochemical cell, with [NADH] = 0.15 mM in the first injection, and an increase of 0.35 mM each time thereafter.

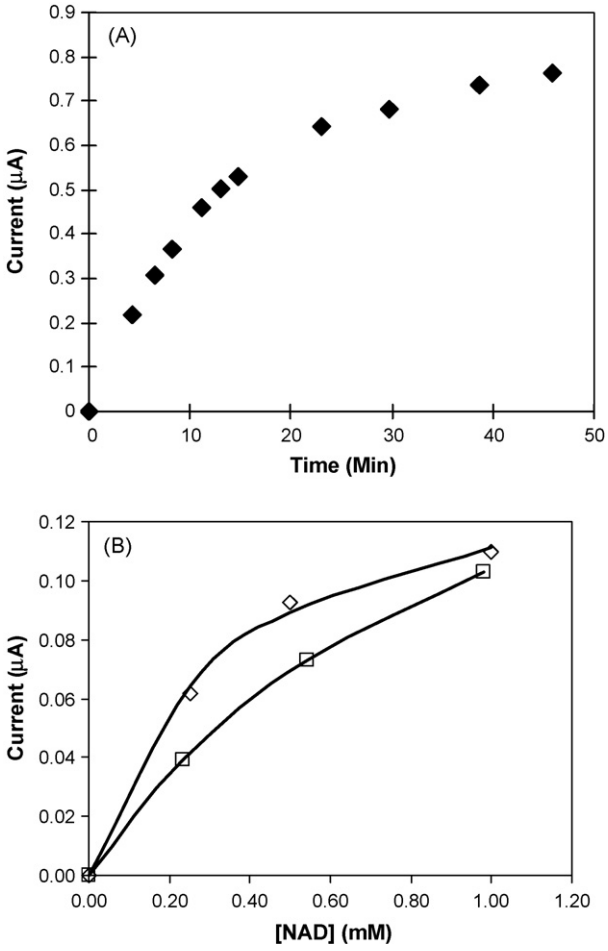


**Fig. 5.** The oxidation reaction of NADH regeneration in a glycerol oxidation reaction system. (A) Time course of the current of NADH from glycerol oxidation reaction in cyclic voltammetric measurements in a non-stirring system. Potential = 0.55 V. Reaction conditions: [Glycerol] = 50 mM; [NAD] = 2 mM; [GlyDH] = 26.7 U/ml in 50 mM $NH_4Cl$–$NH_4OH$ buffer (pH 9.0). (B) Current efficiency of the oxidation of NADH on the CNT–CFME electrode. [Glycerol] = 25 mM, [GlyDH] = 0.24 U/ml, and [NAD] varies from 0 to 1 mM. Empty squares (□): stabilized I-t current reading; empty diamond (◊): current calculated from UV–vis measurement.

Michaelis–Menten kinetic model. When a longer reaction time was allowed, the oxidation current reached a stationary stage. Therefore, data at the point of 20 min were used in subsequent studies for the sake of measurement stability.

To examine the current efficiency of NADH oxidation on the CNT-CFE electrode, the stabilized current readings at 0.55 V on cyclic voltammogram were compared to the currents calculated from NADH oxidation. First, the NADH generation at various NAD concentrations was respectively measured by monitoring NADH absorbance at 340 nm using a UV–vis spectrometer. From the absorbance of NADH at 340 nm, the concentration of NADH generated in the reaction was calculated. The current of oxidation for such an amount of NADH was then determined from the NADH generation rate, with the assumption that one NADH provides one electron to the electrode at the oxidation potential. The calculated theoretical value of currents was used to divide current measurements from cyclic voltammograms to estimate current efficiency at each NAD concentration (Fig. 5B). Results show that the oxidation current at different initial NAD concentrations attained different efficiency levels, ranging from 65% at 0.5 mM of NAD to 93% at 1.0 mM of NAD, indicating that the NADH generated from glycerol oxidation reaction can be nearly completely oxidized on CNT-CFME electrode at an NAD concentration larger than 1.0 mM. This indication signifies the promise for large-scale bioelectrochemical applications by using our CNT-modified cellulose-based carbon fibers as the electrode.

Other than regenerating NADH in large-scale bioelectrochemical applications, the single carbon fiber microelectrode presented in this paper can also be used in biosensors involving enzyme reactions with NAD/NADH as a cofactor. Using glycerol oxidation reactions catalyzed by glycerol dehydrogenase as an example, all three components (glycerol, NAD, and glycerol dehydrogenase) can be measured electrochemically based on the principle of NADH oxidation on CNT-modified carbon fiber microelectrodes. Based on Eqs. (2) and (3), the measured current from the oxidation of NADH on the electrode would indicate the concentration of a component (glycerol, NAD, or glycerol dehydrogenase) if the other two components were provided in excess.

$$\text{Glycerol} + \text{NAD} \xrightarrow{\text{GlyDH}} \text{Dihydroxyacetone} + \text{NADH} \quad (2)$$

$$\text{NADH} \rightarrow \text{NAD} + \text{H}^+ + 2\text{e}^- \quad (3)$$

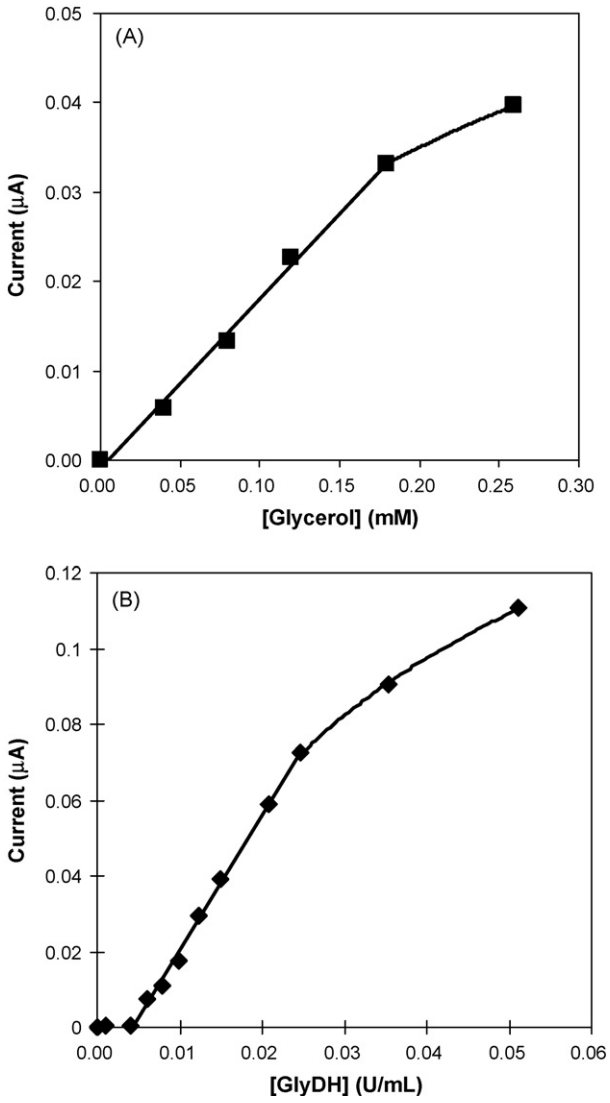


**Fig. 6.** Linear detection ranges of glycerol dehydrogenase and glycerol at a constant NAD concentration (2 mM). (A) Current response in detecting NADH generation in glycerol oxidation reaction as a function of changes in glycerol concentration; [GlyDH] = 0.4 U/ml; (B) current response in detecting NADH generation in glycerol oxidation reaction as a function of changes in glycerol dehydrogenase concentration; [Gly] = 20 mM.

Calibration curves of glycerol and glycerol dehydrogenase at 0.6 V in amperommetry with a constant NAD concentration (2 mM) are shown in Fig. 6. For detecting glycerol, the linear detection range was from 0 to 0.25 mM (Fig. 6A), and the detection limit was 0.04 mM (data not shown). The detection limit of glycerol on this CNT-CFME is the same as the detection limit reported on a NAD modified carbon paste electrode (Álvarez-González et al., 2000). For measuring glycerol dehydrogenase activity, the linear range of measurement (Fig. 6B) was from 0.004 to 0.05 U/ml, and the detection limit was 0.004 U/ml. These figures demonstrate the multiple applications that this kind of CNT-carbon fiber electrodes can be used for. Moreover, for other dehydrogenase enzymes that work with NAD, a broad range of substrates can also be detected with methods similar to the approach in this paper. The benefits of sustainable electrode materials, less amount of samples used, and smaller system setup can also be realized.

## 4. Conclusion

A new method of fabricating hierarchically structured carbon electrodes was reported in this paper by growing carbon nanotubes (CNTs) with carbonization of a renewable material (cellulose) in the presence of metal ions as the catalyst in a high temperature furnace. The process provides a fast approach in the manufacturing of carbon materials for electrochemical applications. The resulting carbon materials were fabricated into carbon microelectrodes and tested in the detection of NADH oxidation. The overpotential of NADH decreased from over 0.8 to 0.6 V for the CNT-modified carbon fiber electrode, indicating that the presence of CNTs could lower the potential of NADH oxidation on carbon electrodes, thereby reducing possibilities of electrode fouling. The single fiber microelectrode is promising for applications such as enzyme, glycerol, and NADH biosensors. Combining with a wide range of dehydrogenase that can be selected to work with NADH, the applications of such a microelectrode can be expanded to include biomedical devices, bioenergy processes, and production of many enzyme-catalyzed products. The carbonization method of cellulose fibers reported is also expected to be an appealing approach for the production of large geometry electrodes suitable for industrial scale electrochemical processes.

## Acknowledgments

The authors would like to thank the University of Minnesota Initiative for Renewable Energy and the Environment (IREE) Program and the Biocatalysis Seed Grant from the Biotechnology Institute for financial supports.

## References

Aguei, L., Yanez-Sedeno, P., Pingarron, J.M., 2008. Anal. Chim. Acta 622 (1–2), 11–47.
Álvarez-González, M.I., Saidman, S.B., Lobo-Castanon, M.J., Miranda-Ordieres, A.J., Tunon-Blanco, P., 2000. Anal. Chem. 72, 520–527.
Amatore, C., Arbault, S., Guille, M., Lemaître, F., 2008. Chem. Rev. 108 (7), 2585–2621.
Amatore, C., Maisonhaute, E., 2005. Anal. Chem. 77 (15), 303A–311A.
Baltes, N., Thouin, L., Amatore, C., Heinze, J., 2004. Angew. Chem., Int. Ed. 43 (11), 1431–1435.
Brunauer, S., Emmett, P.H., Teller, E., 1938. JACS 60, 309–319.
Brett, C.M.A., Brett, A.M.O., 1993. Electrochemistry: Principles, Methods, and Applications. Oxford University Press, New York.
Bruns, D., 2004. Methods 33 (4), 312–321.
Chen, R., Huang, W., Tong, H., Wang, Z., Cheng, J., 2003. Anal. Chem. 75 (22), 6341–6345.
Du, F., Huang, W., Shi, Y., Wang, Z., Cheng, J., 2008. Biosens. Bioelectron. 24 (3), 415–421.
Hayes, M.A., Kuhr, W.G., 1999. Anal. Chem. 71 (9), 1720–1727.
Hou, H., Reneker, D.H., 2004. Adv. Mater. 16 (1), 69–73.
Huffman, M.L., Venton, B.J., 2009. Analyst 134, 18–24.
Jaegfeldt, H., 1980. J. Electroanal. Chem. 110 (1–3), 295–302.
Ju, H., Leech, D., 1997. Anal. Chim. Acta 345, 51–58.
Kim, D.-Y., Nishiyama, Y., Wada, M., Kuga, S., 2001. Carbon 39, 1051–1056.
Kim, J., Grate, J.W., Wang, P., 2008. Trends Biotechnol. 26 (11), 639–646.
Kumar, S.A., Chen, S.-M., 2008. Sensors 8 (2), 739–766.
Li, P., Zhao, Q., Zhou, X., Yuan, W., Chen, D., 2009. J. Phys. Chem. C 113 (4), 1301–1307.
Mano, N., Mao, F., Heller, A., 2003. J. Am. Chem. Soc. 125, 6588–6594.
Moiroux, J., Elving, P.J., 1978. Anal. Chem. 50 (8), 1056–1062.
Nowall, W.B., Kuhr, W.G., 1995. Anal. Chem. 67 (19), 3583–3588.
Peng, S., Shao, H., Hu, X., 2003. J. Appl. Polym. Sci. 90, 1941–1947.
Plaisantin, H., Pailler, R., Guette, A., Daude, G., Pétraud, M., Barbe, B., Birot, M., Pillot, J.P., Olry, P., 2001. Compos. Sci. Technol. 61, 2063–2068.
Polarz, S., Smarsly, B., Schattka, J.H., 2002. Chem. Mater. 14, 2940–2945.
Qu, L., Du, F., Dai, L., 2008. Nano Lett. 8 (9), 2682–2687.
Robinson, D.L., Hermans, A., Seipel, A.T., Wightman, R.M., 2008. Chem. Rev. 108 (7), 2554–2584.
Sgobba, V., Guldi, D.M., 2009. Chem. Soc. Rev. 38, 165–184.
Štulík, K., Amatore, C., Holub, K., Marecek, V., Kutner, W., 2000. Pure Appl. Chem. 72 (8), 1483–1492.
Swamy, B.E.K., Venton, B.J., 2007. Analyst 132, 876–884.
Valcarcel, M., Cardenas, S., Simonet, B.M., 2007. Anal. Chem. 79 (13), 4788–4797.
Vigolo, B., Pénicaud, A., Coulon, C., Sauder, C., Pailler, R., Journet, C., Bernier, P., Poulin, P., 2000. Science 290 (5495), 1331–1334.
Viry, L., Derré, A., Garrigue, P., Sojic, N., Poulin, P., Kuhn, A., 2007. Anal. Bioanal. Chem. 389, 499–505.

Walters, R.R., Graham, J.F., Moore, R.M., Anderson, D.J., 1984. Anal. Biochem. 14, 190–195.
Wang, J., Deo, R.P., Poulin, P., Mangey, M., 2003. J. Am. Chem. Soc. 125 (48), 14706–14707.
Wang, J., Gu, M., Di, J., Gao, Y., Tu, Y., 2007. Bioprocess Biosyst. Eng. 30 (4), 289–296.
Wang, Y., Li, Q., Hu, S., 2005. Bioelectrochemistry 65, 135–142.
Wang, Y., Serrano, S., Santiago-Aviles, J.J., 2002. J. Mater. Sci. Lett. 21, 1055–1057.
Wightman, R.M., 1988. Science 240, 415–420.
Zayats, M., Willner, B., Willner, I., 2008. Electroanalysis 20 (6), 583–601.